# Anatomy of the Ocean Surface Roughness

P.A. Hwang, D.W. Wang, W.J. Teague, and G.A. Jacobs
*Oceanography Division*

**Introduction:** Water waves are the roughness components of the ocean surface. Their presence causes wind drag, which is an important topic of air-sea momentum transfer. From a remote sensing point of view, surface roughness is an important parameter quantifying the scattering of electromagnetic waves (including radar and optical waves). Understanding the ocean surface roughness properties is clearly important to many areas of physical oceanography and ocean remote sensing.

**The Conventional View:** Traditionally, the ocean surface roughness is equated to the mean-square slope of the ocean surface waves. Results from ocean wave research show a logarithmic increase with wind speed of the mean-square slopes computed from well-established spectral models.[1] This result is consistent with the surface roughness data collected by Cox and Munk (referred to as CM hereafter) in slick surface conditions.[2] Although the airborne measurements by CM were conducted more than a half century ago, this data set remains the most comprehensive in terms of the range of wind and wave conditions and the scope of their statistical analysis; they were able to produce coherent slick coverage for wind conditions up to 9 m/s using man-made slicks.

In contrast to the slick cases, the computed mean-square slopes underestimate the surface roughness measured in clean water conditions by a factor of three in medium to high wind conditions (Fig. 1(a)). In most ocean remote sensing applications, this is a serious problem because clean surfaces are encountered more than slick surfaces.

**The Missing Elements:** CM describe that ". . . with 200 gallons of this mixture [of 40 percent used crankcase oil, 40 percent diesel oil, and 20 percent fish oil] a coherent slick 2,000 feet by 2000 feet could be laid in 25 minutes, provided the wind did not exceed 20 miles an hour [8.94 m/s]. . . . " The fact that the man-made slick remains coherent in relatively high wind speed conditions offers an important clue about the missing components of the surface roughness—that the presence of surface slicks damps out not only the small-scale surface waves but also the wave breaking event, which is an important element controlling the ocean wave dynamics. Experiments have shown that wave breaking produces enhanced surface roughness. It remains uncertain about the dynamic range (in terms of the upper bound wavenumber) of the CM optical data. By experimentation, we examine cases with cutoff wavenumbers ranging from $2\pi/0.3$ to $2\pi/0.03$ rad/m. The difference between the measured clean water roughness and the mean-square slope is plotted in Figs. 1(b) to 1(d). An interesting trend that becomes apparent is that the breaking roughness displays a robust power-law wind speed dependence $U^{1.5}$.

To test the hypothesis of multiple components in the ocean surface roughness, we examine a different kind of surface roughness data source—the backscattering radar cross sections of a spaceborne altimeter. Based on our earlier study, it is found that due to the presence of ambient roughness on the ocean surface, the wind-induced surface roughness is related to the function defining the upper bound of the scatter plot of radar cross sections $\sigma_0$ vs wind speeds $U$. The wind-generated roughness as a function of wind speed derived from the TOPEX altimeter is plotted in Fig. 2(a), again showing much larger magnitude than the calculated mean square slope (dashed line). The wind-speed dependence of the breaking roughness of the altimeter data also follows $U^{1.5}$ (Fig. 2(b)).

**Conclusions:** Our recent analysis of ocean surface roughness has led to the conclusion that there are at least three roughness components: the mean-square slope of wind-generated waves, breaking roughness, and ambient roughness. Only the first two components can be related to local wind generation. The former represents the geometric contribution of the wavy surfaces; the latter is a complicated combination of discontinuities and disruptions of the kinematic and dynamic processes associated with wave breaking.

This result has significant implications on the interpretation of ocean remote sensing data, e.g., wind retrieval from altimeter or scatterometer data. Over the years, the analytical calculation of altimeter return from ocean surface cannot produce satisfactory agreement with measurements, and the operational algorithms of wind retrieval rely on empirical functions instead of a physics-based formulation. The discrepancy of the analytical computation can be explained by the failure to account for the ambient component of the ocean surface roughness.

[Sponsored by ONR]



**References**

[1] P.A. Hwang and D.W. Wang, "Directional Distributions and Mean Square Slopes in the Equilibrium and Saturation Ranges of the Wave Spectrum," *J. Phys. Oceanog.* **31**, 1346-1360 (2001).
[2] C.S. Cox and W. Munk, "Statistics of the Sea Surface Derives from Sun Glitter," *J. Mar. Res.* **13**, 198-227 (1954). ■

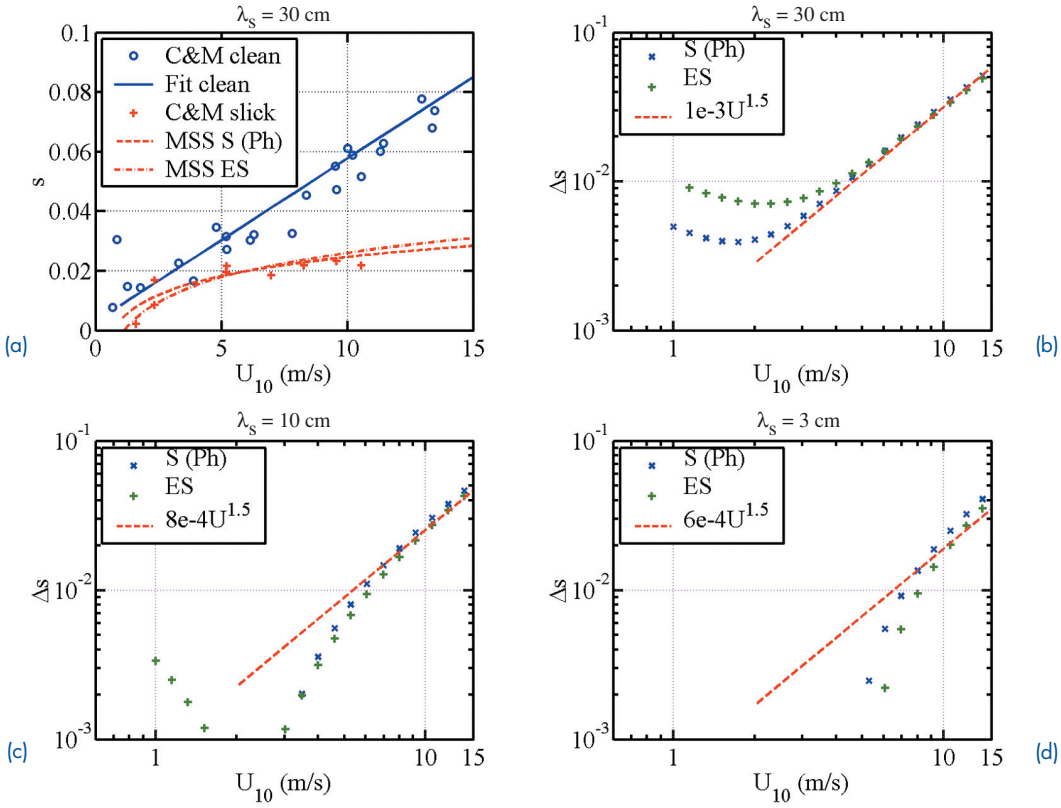


**FIGURE 1**

(a) The ocean surface roughness measured in clean and slick surface conditions (symbols) reported by Cox and Munk[2] and the comparison with calculated mean-square slopes based on established wave spectral models (curves).[1] (b)-(d) Breaking roughness calculated from the difference of the total roughness (clean water condition) and the mean-square slopes assuming three different cutoff wavenumbers.

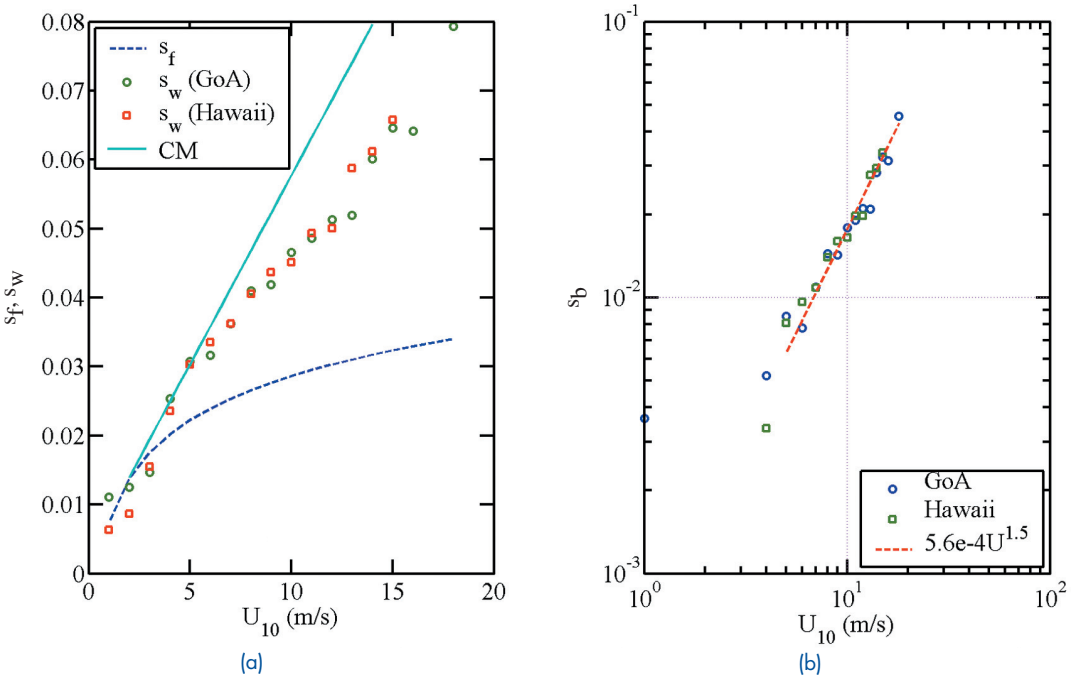


**FIGURE 2**

(a) Wind-induced roughness (symbols) derived from the TOPEX altimeter data. The calculated mean-square slope is shown with the dashed curve; for reference, the best-fit curve representing the CM clean water data is shown with the solid curve. (b) The breaking roughness derived from the altimeter data.

## Nearshore Circulation in Complex Regions

J.M. Kaihatu and W.E. Rogers
*Oceanography Division*

**Introduction:** As ocean surface waves propagate over the continental shelf and break in shallow nearshore areas, their energy is dissipated in the surf zone. The gradients in the waveheights and momentum give rise to the generation of wave-induced nearshore circulation. Wave forcing of circulation in the surf zone is a major cause of sediment transport and beach morphology evolution; its understanding and prediction are essential for military applications such as amphibious landings and mine warfare. Semi-empirical expressions for the nearshore circulation exist over planar bathymetry. However, over more complex bathymetric configurations, such as sandbars, rip channels, and canyons, numerical models are required for comprehensive descriptions of the wave-driven flow. Most of these extant numerical models either use irregular wave forcing but simplify the hydrodynamics (as is the case for nearshore circulation models in the operational Navy), or allow more involved hydrodynamic formulations but reduce the forcing to that of monochromatic wave theory. Either modeling option can potentially lead to nearshore hydrodynamic predictions that do not exhibit the variability seen in nature.

**Numerical Modeling of Nearshore Circulation:** Recently, the Naval Research Laboratory (NRL) developed significant modifications to a sophisticated quasi-three-dimensional (quasi-3D) numerical hydrodynamic model. This model, SHORECIRC, was developed by Dr. Ib Svendsen and students at the Center for Applied Coastal Research of the University of Delaware. It is "quasi-3D" in that it actively models the depth-averaged horizontal velocities, but uses sophisticated analytic expressions to calculate the vertical profile of these horizontal velocities. The model is therefore able to simulate the evolution of horizontal velocities of the nearshore circulation field (including the depth-varying offshore flow, or "undertow") in all three dimensions (and time) without large computational effort. However, its physical mechanisms were geared toward monochromatic (single frequency) wave forcing, and thus are not applicable to field cases where waves of many frequencies and directions are present. NRL performed the reformulation of these physical mechanisms by adopting a probability distribution of waveheights inside the surf zone, and then integrating existing monochromatic formulations over this distribution. The resulting model represents the first implementation of random wave forcing in a general quasi-3D hydrodynamic model, thus allowing direct application to field situations.

**Application to Nearshore Canyon:** A major nearshore measurement campaign for the 2003-2004 time frame will be conducted near the Scripps Institution of Oceanography in La Jolla, California. This field experiment will be a collaborative effort among several universities and research institutions, including NRL. The site of the experiment is located at the head of Scripps Canyon, a major undersea canyon that exerts a strong polarizing effect on the nearshore wave and circulation climate. Figure 3 shows an aerial photograph of Black's Beach, located at the head of Scripps Canyon, taken by Dr. Steve Elgar of Woods Hole Oceanographic Institution. The

**FIGURE 3**
Aerial photograph of Black's Beach, north of Scripps Canyon in California. The undersea canyon enacts a strong variability on the nearshore wave and circulation environment. Arrows trace the presumed longshore and rip current patterns. Photo courtesy of Dr. Steve Elgar, Woods Hole Oceanographic Institution.

high variability in the wavefield and complex rip current environment is evident.

NRL developed a nested modeling system to investigate the possible nearshore flow patterns at this site, using the reformulated SHORECIRC model at the finest nest. The coastal-scale wave model SWAN (developed at Delft Technical University) propagated offshore wave energy into the nearshore canyon site. Figure 4 shows the waveheight prediction from SWAN over the entire domain, which was resolved at ~30 m in both directions. Information from SWAN was then input to a high-resolution nearshore irregular wave model (REF/DIF-S, developed at the University of Delaware) for simulating wave propagation over the small area in the white box near Black's Beach (at ~4-m resolution in both directions). The high-resolution wave model results were then used for forcing in the reformulated SHORECIRC model. Figure 5 shows the predicted average nearshore circulation pattern. The pair of northward-directed rip currents qualitatively represents what is seen in Fig. 3. No attempt was made to simulate the exact condition depicted in Fig. 3, so the rip current pair is probably more a direct result of the complex bathymetry than the wave climate offshore of the domain, and thus is likely to be a persistent feature.

**Summary:** NRL has developed significant modifications to the quasi-3D hydrodynamic model SHORECIRC. The most essential of these modifications (irregular wave forcing) enables the modeling of nearshore circulation without gross simplification of actual conditions. NRL developed a nested modeling system for the Scripps Canyon area, the site of an upcoming measurement campaign, and used this system to investigate potential flow conditions in the area. The presence of a rip current pair in the results qualitatively agrees with observations in the area. The NRL-enhanced SHORECIRC model shows promise as a forecasting tool, and further model validation is aimed toward this evaluation.

[Sponsored by ONR]

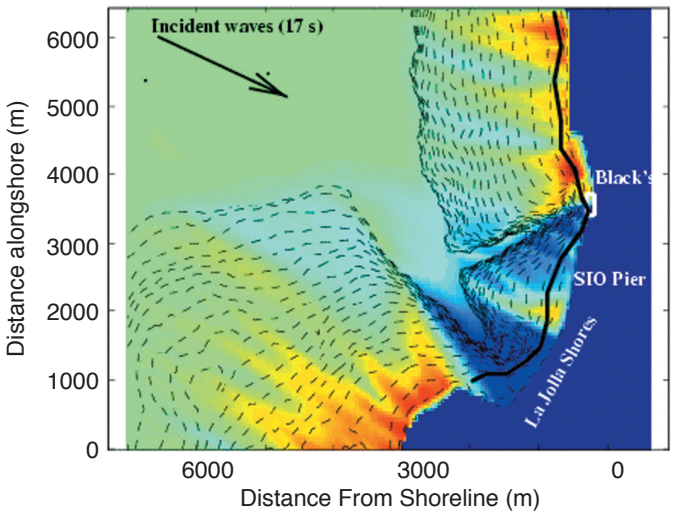


**FIGURE 4**
NRL model nest at Scripps Canyon: waveheights from the SWAN wave model over the shelf area near Scripps Canyon and Black's Beach. North is upward. Wave spectra with offshore height of 2 m and peak period of 17 s approach from the northwest. Waveheights over the domain range from 4 m (darkest red) to 0.25 m (deepest blue). Results are input into high-resolution wave and hydrodynamic models near Black's Beach (white rectangle).

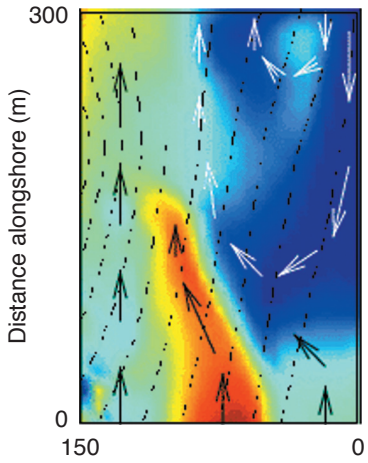


**FIGURE 5**
NRL model nest at Scripps Canyon: predicted nearshore circulation pattern at Black's Beach from NRL-modified SHORECIRC model. Colors denote magnitude of longshore (north-south) velocities; range is from 1 m/s northward (dark red) to 1 m/s southward (deep blue). Arrows denote nearshore circulation pattern. Rip current pair (white arrows) are persistent features in simulations in this area, thus suggesting strong bathymetric influence on current patterns and milder sensitivity to nature of offshore conditions.

## Remote Wind Connections to Strait Transports

G.A. Jacobs, H.T. Perkins, R.H. Preller, H.E. Ngodock, W.J. Teague, S.K. Reidlinger, D. Ko, and J.W. Book
*Oceanography Division*

**Introduction:** NRL's Oceanography Division research is providing new understanding of the mechanisms controlling flow through the Korea Strait. Located between Korea and Japan, the strait is the critical juncture between the East China Sea, the Yellow Sea, and the Sea of Japan. The Korea Strait transport provides the largest portion of horizontal heat and salt flux into the Sea of Japan. The strait transport forms a relatively warm fresh surface layer in the summer and strengthens the anticyclonic circulation south of the subpolar front. Understanding the fundamental dynamics controlling transport through the strait is crucial to developing environmental monitoring and prediction systems for Navy applications. The area is challenging for making direct observations as well as for numerical modeling. The successful deployment of 12 acoustic Doppler current profilers (ADCP) (Fig. 6), the reproduction of observed transport variations by the Navy Coastal Ocean Model (NCOM) (Fig. 7), and sensitivity provided by the numerical adjoint (Fig. 8) are significant achievements. They are leading to an improved understanding of the dynamics controlling the area, and this understanding guides the continued development of Navy environmental prediction systems.

**Trawl-resistant Bottom Mounts:** In situ current measurements have been limited in this area because of the high regional fishing activity. Extensive bottom trawling endangers conventional moorings deployed for more than just a few days. To counter this problem, NRL in conjunction with NATO's SACLANT Research Centre developed trawl-resistant bottom mounts (TRBM) to contain the ADCP instrument (Fig 6). Instrument sensors that record orientation indicate encounters with fishing activities by many of the 12 ADCPs deployed in the strait from May 1999 through March 2000. In spite of the interference, the instruments provided excellent coverage. Such an extensive array over such a long time period has never been achieved in this area. These data are providing extensive new understanding of the dynamics controlling exchanges between the Asian marginal seas.

**Numerical Modeling:** NRL has been developing NCOM, which is an evolution of previous ocean models. NCOM is designed to represent circulation on the continental shelf and the deep ocean more accurately by combining the unique methods previous ocean models used to represent features in these different regions. The model used in this project covers the Asian marginal seas from the South China Sea through the Sea of Japan so that the connections between the seas can be examined. The horizontal resolution used in the examples here is 1/8°. The eastern boundary conditions are provided by a larger North Pacific model that assimilates satellite sea level and temperature measurements. Wind forcing is provided by the Navy Global Atmospheric Prediction System (NOGAPS), and the model is run from 1997 through 2000. Wind forcing in the synoptic band (2 to 20) days is expected to produce a deterministic transport response through the strait. The model and observed synoptic transports compare well (Fig. 7).

**Sensitivity through Adjoints:** The numerical model dynamical equations represent the physics governing ocean circulation. The good comparison between the model and observed synoptic transports indicates that the wind forcing and the model dynamics connecting the wind forcing to the transport are both good. However, the numerical model does not provide an immediate indication of the area over which wind stress is most important to forcing the strait transport. While carefully designed numerical model experiments may be performed to provide this insight, the adjoint of the model gives a more direct answer. The adjoint is a method that provides the derivative of a model output (such as the transport through the strait) with respect to the model inputs (such as the wind forcing). NRL is presently constructing numerical model adjoints to understand ocean dynamics and assimilate measurements into models.

The strait transport sensitivity to wind stress at a time lag of 3 h (Fig. 8) indicates that the southerly wind stress off the east Korean coast is most influential. A slightly less sensitive area for transport through the strait lies directly south of the strait. Counterintuitively, wind stress across the relatively shallow Yellow Sea shelf is not a large contributor to the strait transport. The physical mechanism connecting the regions of wind influence to the strait transport is the propagation of oceanic Kelvin waves. An observer moving with the wave would have the coast on their right-hand side when facing the direction of propagation. Wind-generated Kelvin waves in the Yellow Sea propagate away from the Korea Strait, taking the wind information to the Taiwan Strait; Kelvin waves generated in the Sea of Japan propagate along the Korea coast to the Korea Strait.

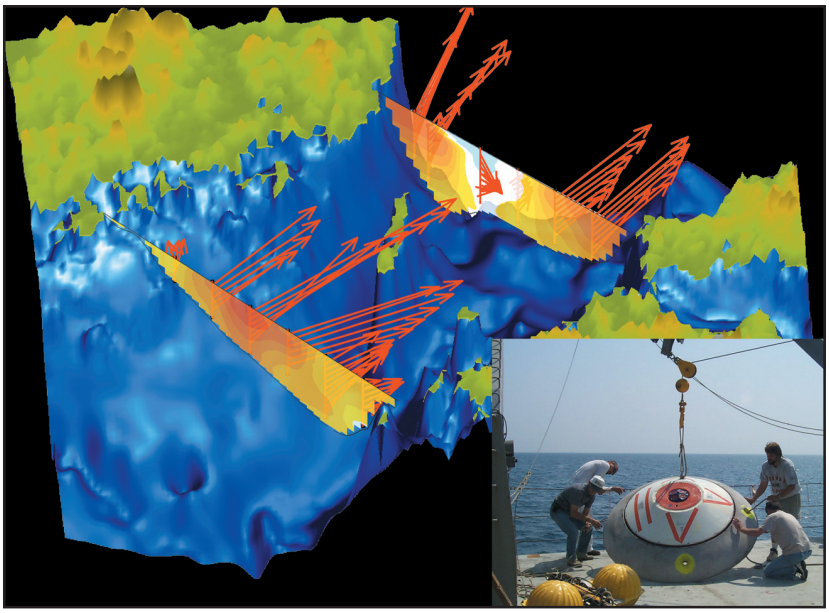

**FIGURE 6**
Twelve bottom-mounted ADCPs were deployed in trawl-resistant bottom mounts between Korea and Japan. Red arrows represent the mean velocities at different depth levels for each mooring. Colored sections represent the mean transport across each section.

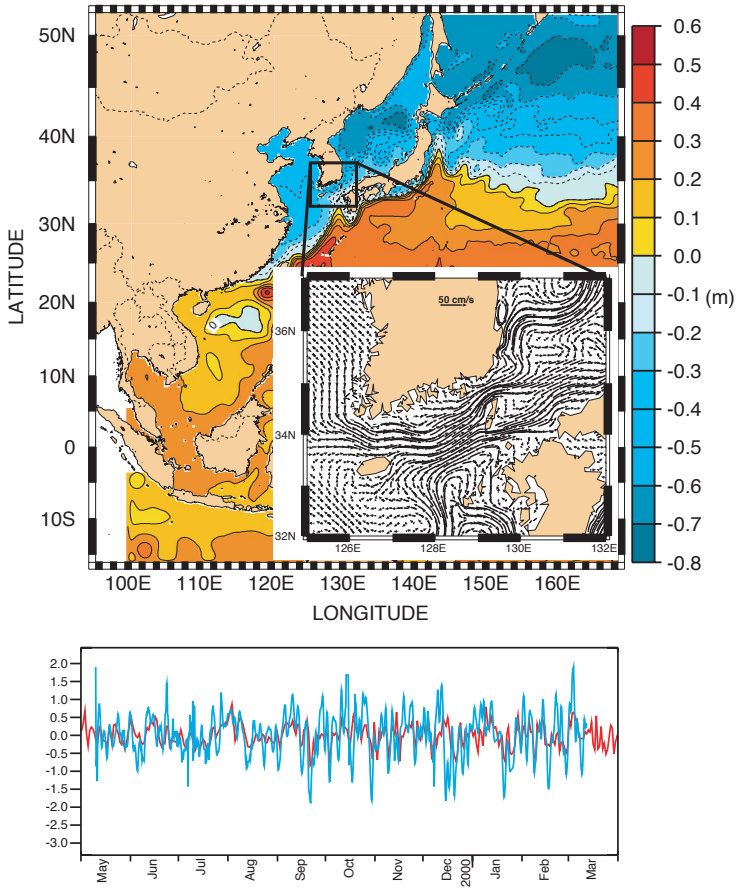


**FIGURE 7**
The NRL Coastal Ocean Model (NCOM) is set up for this experiment to cover all the Asian marginal seas at 1/8° resolution. The general circulation of the region may be viewed by the sea level (flow generally following lines of constant height, which is represented by the color contours). The model also reproduces the local features of circulation such as the transport through the Korea Strait. The synoptic transport (bottom) observed by the instruments (red line) and reconstructed by the numerical model (blue line) are in good agreement.

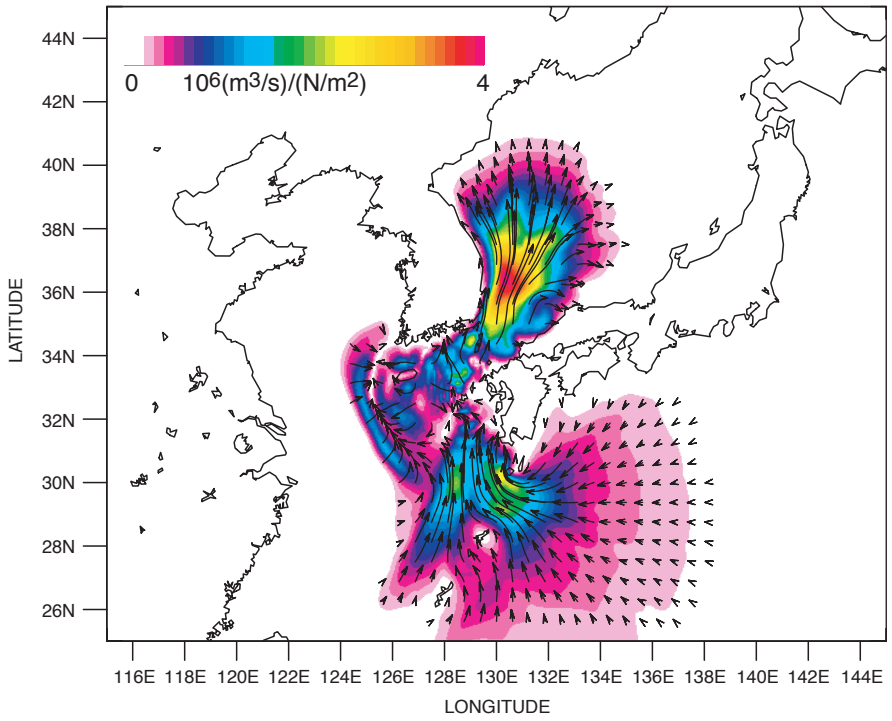


**FIGURE 8**
The adjoint model provides an estimate of the sensitivity of the strait transport to the wind stress (displayed here at a 3-h lag). The color indicates the amplitude and vectors indicate direction. The transport through the Korea Strait is most sensitive to the wind stress across the area east of the Korea peninsula and less sensitive to the area south of the strait.

**Using Knowledge to Build Systems:** Knowledge of the dynamics controlling exchanges between the interconnected seas is needed to build accurate monitoring and prediction systems. Evaluation through in situ measurements is crucial for confidence in any system. Understanding the model sensitivity is required to know where efforts must be concentrated to provide the maximum payoff. All these research issues are leading to improved operational capability. NCOM is presently being implemented in a global 1/8° system to provide surface currents and temperatures throughout the world.

**Acknowledgments:** This work is supported by the NRL 6.1 Dynamical Linkage of the Asian Marginal Seas (LINKS) and the NRL 6.1 Error Propagation on the Continental Shelf (EPIC) projects.

[Sponsored by NRL]

## Laboratory for Underwater Hydrodynamics

J. Grun,[1] T. Jones,[1] C. Manka,[2] and L.D. Bibee[3]
[1]*Plasma Physics Division*
[2]*Research Support Instruments*
[3]*Marine Geosciences Division*

**The LUH:** The Laboratory for Underwater Hydrodynamics (LUH) is an indoor laboratory facility designed to provide a well-controlled and a well-diagnosed environment for the performance of precise, small-scale hydrodynamics experiments for the Navy (Fig. 9). In the LUH, underwater shocks and bubbles are generated by the rapid heating of a small volume of water or solid material inside a pressurized water tank by a short and powerful (5-ns duration, 500-J energy) laser pulse focused to a small spot inside the tank. Upon being heated, the small volume of water or other material turns to gas and expands, thereby forming a bubble and generating the pressure for launching a shock. Cavitation bubbles that are generated by this mechanism have kilobar pressures at centimeter distances; unlike bubbles formed by explosives, they are visually transparent, allowing diagnosis of the inside of the bubble. The laser focusing optics can be set up to create a point-shaped focus, a disk-shaped focus, or a line-shaped focus useful for simulating the behavior of different shapes of charges, including a line charge.

Besides containing water, the tank holds objects scaled to model underwater structures or surfaces of interest to the Navy. One of these objects is a large tray with a porous bottom designed to hold up to 20-cm deep sand. This water flow and sand tray are designed to model littoral water and beach conditions. De-aired, gas-saturated, or super-saturated water can be pumped through the porous bottom of the sand tray, thereby changing the air content of the sand over the full range observed in natural environments. The chamber can also be pressurized to 2

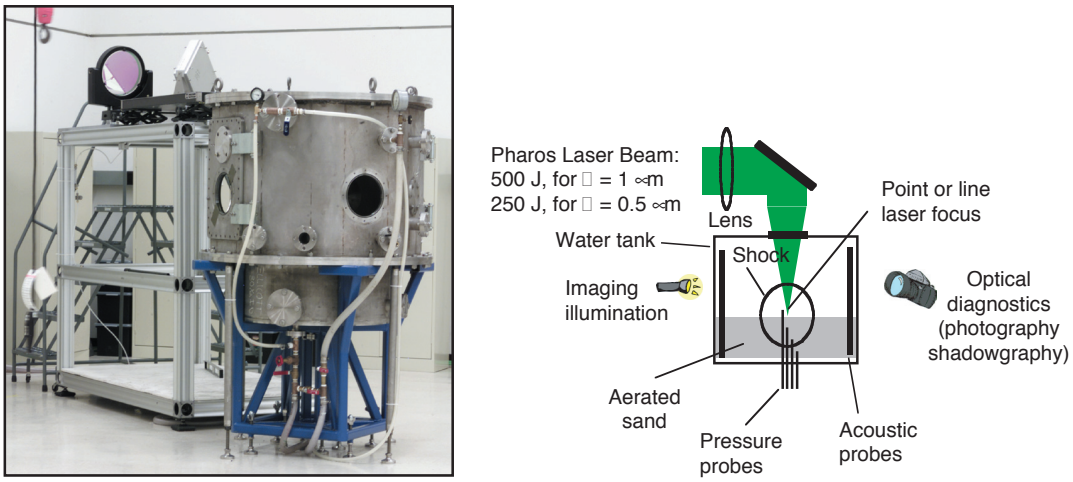


**FIGURE 9**
The NRL Laboratory for Underwater Hydrodynamics.

atmospheres or partially depressurized to 0.1 atmosphere to simulate conditions at various depths.

The LUH facility is equipped with a large number of state-of-the-art diagnostics, such as high-speed imaging (500 frames at 200,000 frames/second), Schlieren shadowgraphy, time-resolved interferometry, spectroscopy, and miniature fiber-optic or electric pressure gauges. Range gating is used to image through murky water.[1] Sand conditions are diagnosed with sand core samplers and geo-acoustic probe arrays capable of producing tomographic, three-dimensional images of sand/air content (Fig. 10).

In constructing the LUH facility we took advantage of previous experiments that used nonexplosive methods to generate underwater shocks or cavitation. Among them are interesting experiments that used lasers 5,000 times less energetic than ours to study shock hydrodynamics associated with ocular laser surgery.[2] We also considered using spark-generated shocks and bubbles,[3] but chose to use a laser instead because it does not require the use of electrodes, which may interfere with bubble dynamics.

**Sample Results:** Experiments performed thus far on the LUH include propagation of ultra-short (picosecond) laser light pulses through water, free-field shock and bubble dynamics, bubble-jet formation near a rigid boundary, shock transmission through a gas channel in water, and interaction of line-charge-like cylindrical shocks and point-charge-like spherical shocks with sand containing different amounts of air. Results of these experiments were used to help validate DYSMAS and GEMINI, the Navy's main predictive hydrodynamics and materials codes, which are run by the Naval Surface Warfare Center at Indian Head, Maryland.

Figure 11 shows an example of the experimental results that LUH produces, cavitation bubbles with

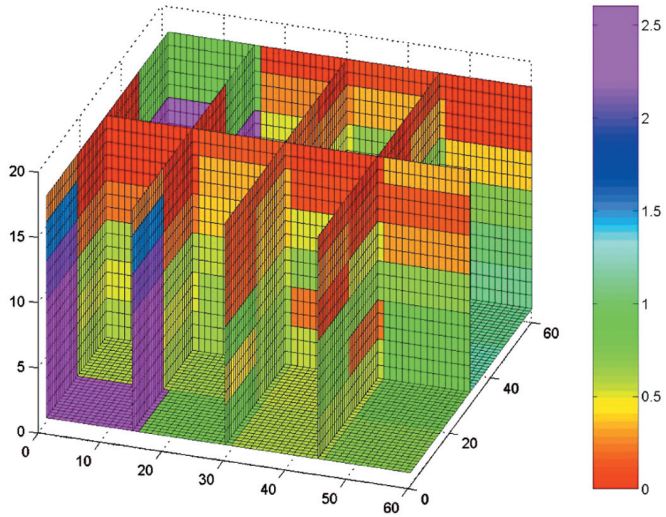


**FIGURE 10**
Tomographic reconstruction provides a precise three-dimensional image of the air content in the sand tray. The air content in this sample varies from 1% at the bottom to 0% at the top.

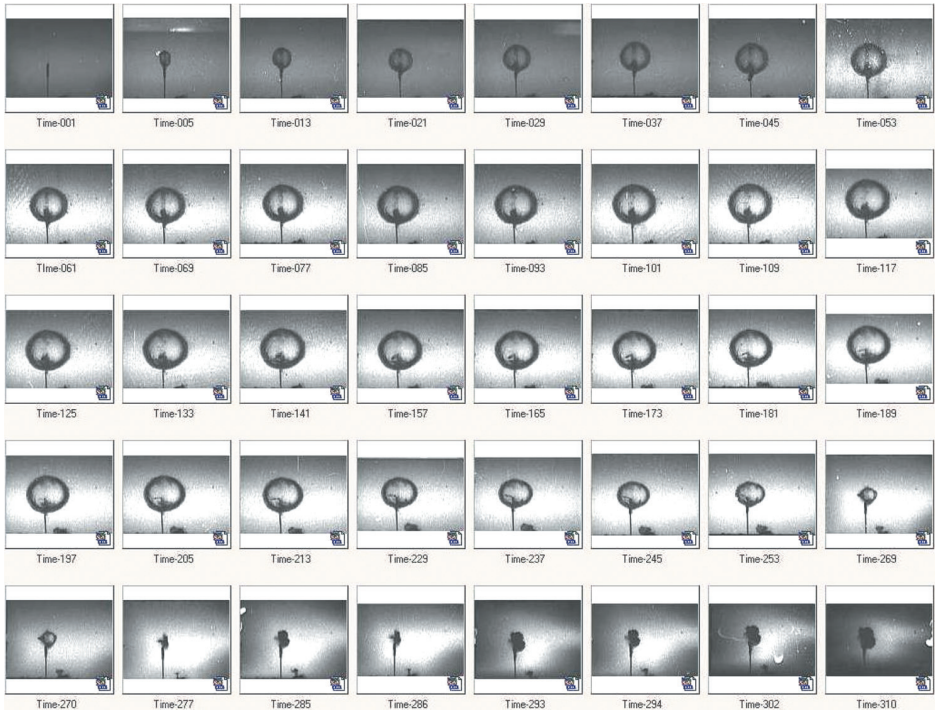


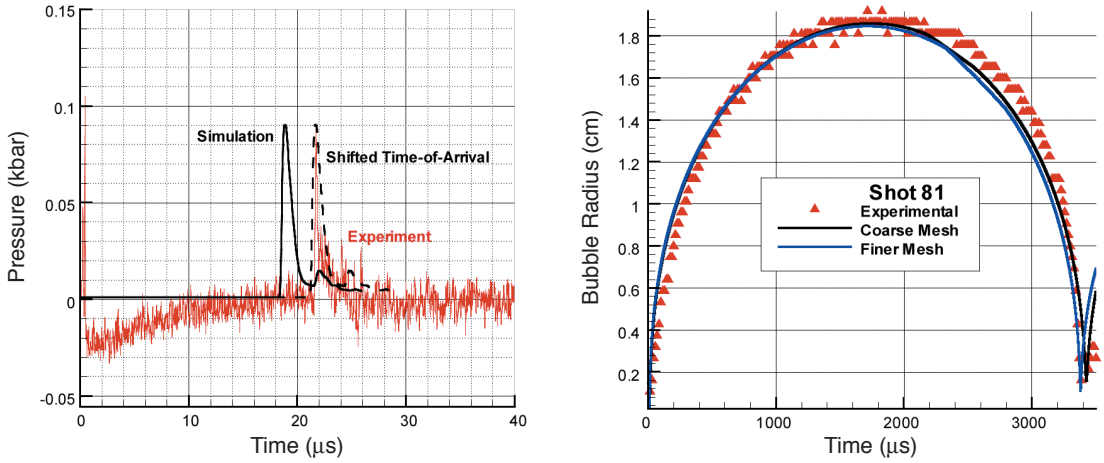


**FIGURE 11**
Every eighth image of the evolution of a bubble formed by a laser and a comparison of experimental and computational shock pressure time history and bubble dynamics.

no boundary present and a comparison to DYSMAS simulations. Here, a laser-generated bubble is photographed using high-speed imaging. The images (every eighth one is presented) show a thin piece of plastic being held on a stalk in water. The laser pulse heats this plastic, vaporizing it so that it expands, forming the bubble that is just beginning to appear in the first frame. The bubble in the image sequence is seen to expand, collapse, and then rebound again before the experiment is concluded. A DYSMAS simulation of the bubble formation shows an almost perfect match between the measured and calculated bubble trajectory.

**Acknowledgments:** The experiments performed on the LUH are designed and interpreted jointly with the Naval Surface Warfare Center in Indian Head, Maryland, in particular with Drs. Alexandra Landsberg, Daniel Tam, and Gregory Harris. The authors also thank Dr. Judah Goldwasser of ONR for his encouragement and support.

[Sponsored by ONR]

**References**

[1] E.A. Mclean, H.R. Burris, and M.P. Strand, "Short-pulse Range-gated Optical Imaging in Turbid Water," *Applied Optics* **34**, 4343-4351 (1995).

[2] W. Lauterborn and H. Bolle, "Experimental Investigations of Cavitation-bubble Collapse in the Neighborhood of a Solid Boundary," J. Fluid Mech. **72**(2), 391-401 (1975).

[3] G.L. Chahine, G.S. Frederick, C.J. Lambrecht, G.S. Harris, and H.U. Mair, "Spark-generated Bubbles as Laboratory-scale Models of Underwater Explosions and Their Use for Validation of Simulation Tools," *Proceedings of 66th Shock and Vibration Symposium*, Biloxi, MS, Vol. 2, pp. 265-276 (1995) (available from the Shock and Vibraton Analysis Center <http://SAVIAC.USAE.BAH.com>).